Mineralogical Magazine, December 2004, Vol. 68(6), pp. 871–885

Euhedral crystals of ferroan platinum, cooperite and mertieite-II from alluvial sediments of the Darya river, Aldan Shield, Russia

G. G. Shcheka[1,2,*], A. N. Solianik[1], B. Lehmann[2], A. Bieniok[3], G. Amthauer[3], D. Topa[3] and J. H. G. Laflamme[4]

[1] Far East Geological Institute, Russian Academy of Sciences, 159 Prospect 100-letya, Vladivostok 690022, Russia
[2] Institute of Mineralogy and Mineral Resources, Technical University of Clausthal, Adolph-Roemer-Strasse 2a, D-38678 Clausthal-Zellerfeld, Germany
[3] Institute of Mineralogy, University of Salzburg, Hellbrunnerstrasse 34, A-5020 Salzburg, Austria
[4] Mining and Mineral Sciences Laboratories, Canada Centre for Mineral and Energy Technology, 555 Booth Street, Ottawa, Ontario K1A 0G1, Canada

ABSTRACT

Idiomorphic crystals (up to 3.5 mm) of ferroan platinum, cooperite and mertieite-II were found in a heavy-mineral concentrate from stream sediments of the Darya river in the Aldan Shield, Russia. Pt-Fe crystals display cubic and thin platy habits; occasionally they are twinned. The chemical composition ranges from $Pt_{2.64}Fe_{1.00}$ to $Pt_{2.88}Fe_{1.00}$ with Os, Ru, Ir, Rh and Pd below the analytical detection limit of the electron microprobe. X-ray diffractometry of Pt-Fe crystals suggests a F-centred cubic lattice, characteristic of ferroan platinum. Some of the ferroan platinum crystals have large (about 100 μm wide) cooperite overgrowth rims or are covered by a Au-Ag alloy. Cooperite also occurs as large euhedral crystals (up to 3 mm across, partly twinned). Crystals of mertieite-II are speckled with μm-sized (2–5 μm) inclusions of sperrylite and intergrown with minerals of cooperite-braggite solid solution, Pt-Pd-Hg alloy, keithconnite and Au-Ag alloy. Fractures along crystallographic planes of the mertieite-II crystals are filled with Pd-Pt-Fe-Sb-As-Hg-Te-Bi-bearing oxides. The coarse-grained PGM from the Darya have a geological setting similar to the Kondyor PGE placer 75 km to the northeast and are probably related to clinopyroxenite-hornblende-magnetite units of Alaskan-/Uralian-type intrusions.

Keywords: ferroan platinum, cooperite, mertieite-II, PGE oxides, Au-PGE placer, Darya, Aldan Shield, Russia.

Introduction

The Darya Au-PGE placer is located within the southern margin of the Aldan Shield, which is a protrusion of Precambrian basement at the south-eastern part of the Siberian platform (Fig. 1). It is known for numerous PGE deposits and occurrences genetically related to zoned ultramafic-alkaline massifs of Uralian-Alaskan-type, such as Kondyor†, Inagli, Chad, Sibakh (Rozhkov *et al*., 1962; Gurovitch *et al*., 1994; Nekrasov *et al*., 1994; Malitch, 1999). The Kondyor placer is most widely known for its production of ~4 t PGE/year (Platinum 2004, Johnson Matthey) and for its uniquely large (from mm up to 1.5 cm) euhedral ferroan platinum and zvyagintsevite crystals (Sushkin, 1995; Cabri and Laflamme, 1997; Szymañski *et al*., 1997; Shcheka *et al*., 2004) . The Darya river, 75 km SW of Kondyor, was recently explored for alluvial PGE and gold. A field expedition in summer 2001 recovered a heavy-mineral concentrate from the Darya river with pyroxene, amphibole, Fe-Ti-oxides, zircon, gold and PGM. The PGM assemblage is largely

* E-mail: Shcheka@email.com
DOI: 10.1180/0026461046860225
† The English transliteration of the Russian name "Кондёр" has two variants: Konder and Kondyor (see Cabri and Laflamme, 1997). Kondyor is closest to the Russian pronounciation and is preferred here, as in other recent publications.

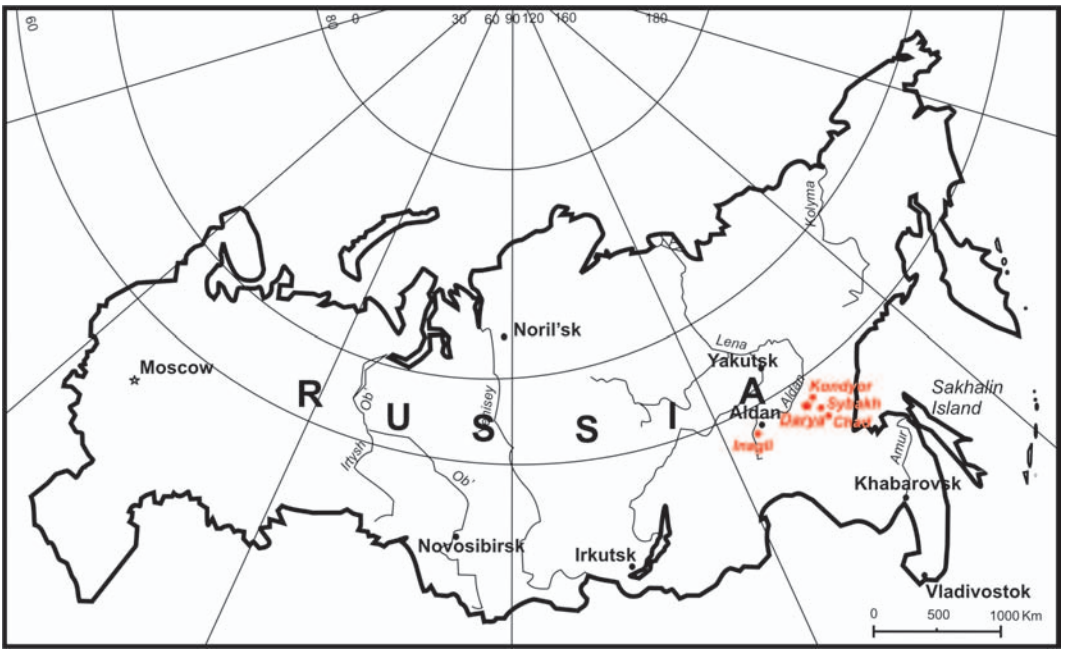

FIG. 1. Location of the Darya river area.

represented both by xenomorphic Pt-Fe alloy grains and by euhedral crystals. The PGE minerals of the Darya placer were briefly described by Mochalov (2001) who documented the occurrence of low-Ir Pt-Fe alloy, and crystals of sperrylite and cooperite. The present manuscript is dedicated to the investigation of some mm-sized PGM grains with euhedral outline. Thirty grains were selected from a heavy-mineral concentrate for detailed mineralogical study, and euhedral crystals of Pt-Fe alloy, cooperite and mertieite-II were identified. This is the first occurrence of mm-sized idiomorphic mertieite-II crystals, and the second occurrence of coarse-grained euhedral ferroan platinum and cooperite crystals. Here we report on the morphology, chemical composition and X-ray data for these unusual crystals.

Geological setting

The Darya alluvial Au-PGE placer is located in the Khabarovskiy Krai province (Siberia, Russia) (Fig. 1). It occurs in the right tributary of the Darya river which is in the western part of the Omninsko-Batomskiy uplift, SE Aldan Shield (Fig. 2; coordinates: 57º 23′ NL and 133º 23′ EL), 75 km SW of the well known Kondyor PGE placer. The Omninsko-Batomskiy uplift has undergone repeated tectonic and magmatic reactivation with multiple intrusive complexes of positive morphostructures (Kondyor, Inagli, Chad, Sibakh). Numerous small stock-like ultramafic bodies are also known (El'yanov and Andreev, 1991). The age of this magmatic activity is obscure (Nekrasov *et al*., 1994). The nearby Kondyor intrusive complex and PGE mineralization was the subject of several radiometric studies: Malitch and Thalhammer (2002) and Pushkarev *et al*. (2002) defined the Os isotope composition of inclusions of Os-Ir alloy in xenomorphic Pt-Fe alloy and found a $^{187}Os/^{188}Os$ ratio of 0.1250±0.002 (n = 5) which gives a mantle model age of 330±30 Ma. Biotite from cross-cutting dykes yielded an $^{40}Ar/^{39}Ar$ age of 120±1 Ma (data by G.K. Czamanske, given by Cabri *et al*. 1998). Pushkarev *et al*. (2002) measured K-Ar ages on biotite of 132±8 Ma and 115±6 Ma for ultramafic and gabbro units, respectively, and a discordant Rb-Sr age of 123±2 Ma for pyroxenite and 93±47 Ma for gabbro-pegmatite, respectively.

A heavy-mineral concentrate was taken from the right tributary of the Darya river (Fig. 3). The creek bed exposes alkaline clinopyroxenite which also occurs in boulders. Reconnaissance mapping

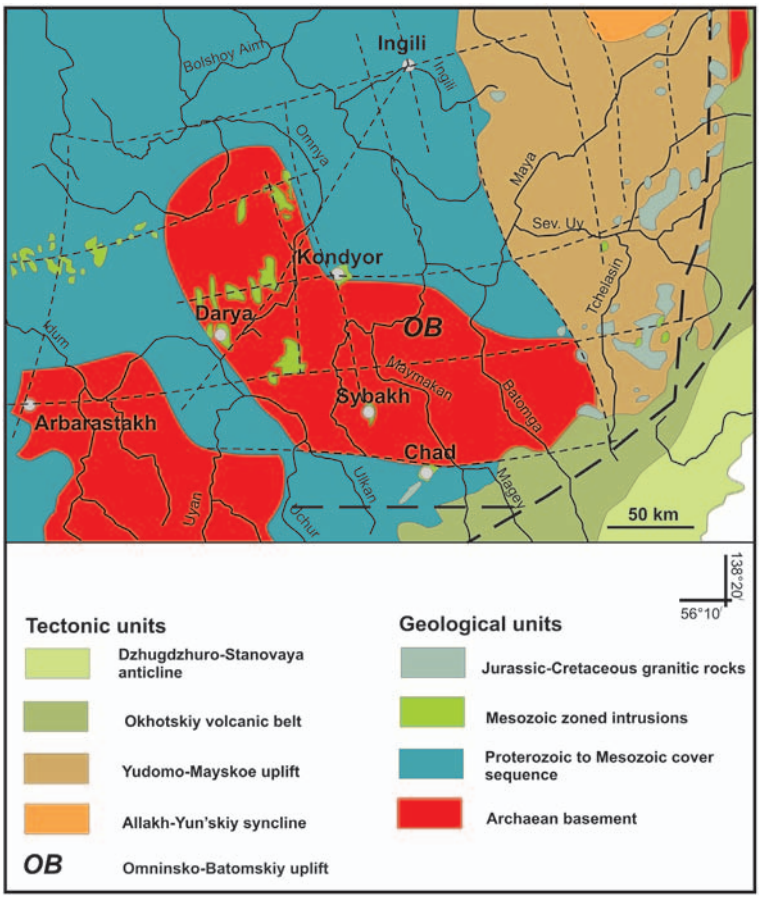

FIG. 2. Geotectonic sketch map of the southeastern Aldan Shield (simplified from El'yanov *et al*., 1991).

defines a circular intrusion with a diameter of 1.2–1.5 km, hosted in updomed Archaean gneisses surrounded by Upper Proterozoic sandstones with abundant sills, dykes and subvolcanic bodies of alkaline and felsic rocks. The clinopyroxenite is medium to coarse grained (pegmatoidal) and consists of aegirine-augite and biotite. Apatite, Ti-rich garnet and Ti-magnetite are present as accessory minerals. There are also many boulders and pebbles of magnetite-rich clinopyroxenite ('koswite') with ilmenite, apatite and kaersutite. The clinopyroxenite from Darya is similar to that of the Kondyor dyke complex (Nekrasov *et al*., 1994).

Analytical techniques

Selected grains were mounted as SEM stubs in order to study their morphology and to obtain preliminary qualitative analyses with the help of a scanning electron microscope (SEM) equipped with an energy-dispersive X-ray spectrometer (EDS). The next step was the preparation of polished sections for electron microprobe analysis by a CAMECA SX100. Three samples were selected for X-ray diffraction (XRD) analysis. Both scanning electron analysis and quantitative wavelength-dispersive electron-microprobe analyses were carried out at the Technical University of Clausthal, Germany. The PGM were analysed at 20 kV, with a beam current of 20 nA and a beam size of ~1 μm. The counting times varied from 10 to 30 s. Eleven to 15 elements were determined by several programs using the following standards: FeS_2, SnO_2, InAs, $CuFeS_2$, InSb, PbTe, HgTe and pure osmium, ruthenium, rhodium, palladium, silver, antimony, gold, platinum, iridium, nickel, iron and copper. The X-ray $K\alpha$ lines were used for

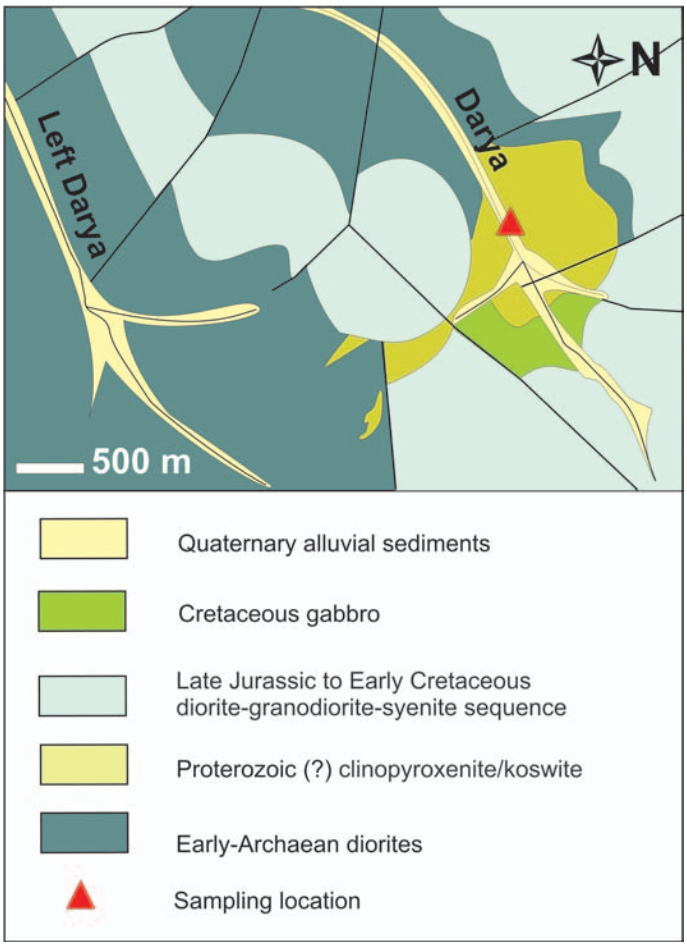

FIG. 3. Geological map of Darya river area.

Ni, Fe; $L\alpha$ for Ru, Rh, Sn, Sb, Au, Pt, Ir, Cu; $L\beta_1$ for Pd and Ag; and $M\alpha$ for Os in the program created for Pt-Fe-S compounds.

Additional microanalysis was done at CANMET, Ottawa, on a JEOL 8900 electron microprobe operated at 20 kV, with a specimen current (cup reading) of 20 nA. The following X-ray lines (and standards) were used: Pd-$L\alpha$ and Sb-$L\alpha$ (Pd_8Sb_3); Cu-$K\alpha$, Ni-$K\alpha$, Ir-$L\alpha$, Te-$L\alpha$ and Bi-$M\alpha$ (metals); As-$L\alpha$ (InAs); Pt-$L\alpha$ and Fe-$K\alpha$ (PtFe); Sn-$L\alpha$ (PtSn). Counting time was of the order of 40 s for the minor and trace elements, and raw data corrections for ZAF were applied.

X-ray analysis of mertieite was carried out with a Philips PW 1060 powder diffractometer with Bragg-Brentano setup, Cu-$K\alpha$, secondary graphite monochromator operating at 40 kV and 20 mA, at the Institute of Earth Sciences, University of Tübingen, Germany, and at the Institute of Mineralogy, University of Salzburg, Austria, using a single-crystal diffractometer with a CCD-area detector (Bruker Smart Apex, Mo-$K\alpha$, primary graphite monochromator operating at 50 kV and 30 mA). The latter was also used for XRD analysis of ferroan platinum alloy.

Morphology, chemical composition and structure of the PGM crystals

Pt-Fe alloy

Most of the 30 idiomorphic PGM crystals selected for this study are Pt-Fe alloy (60%). This mineral phase forms relatively large crystals (up to 3.5×1.5 mm in size) with thin platy or elongated

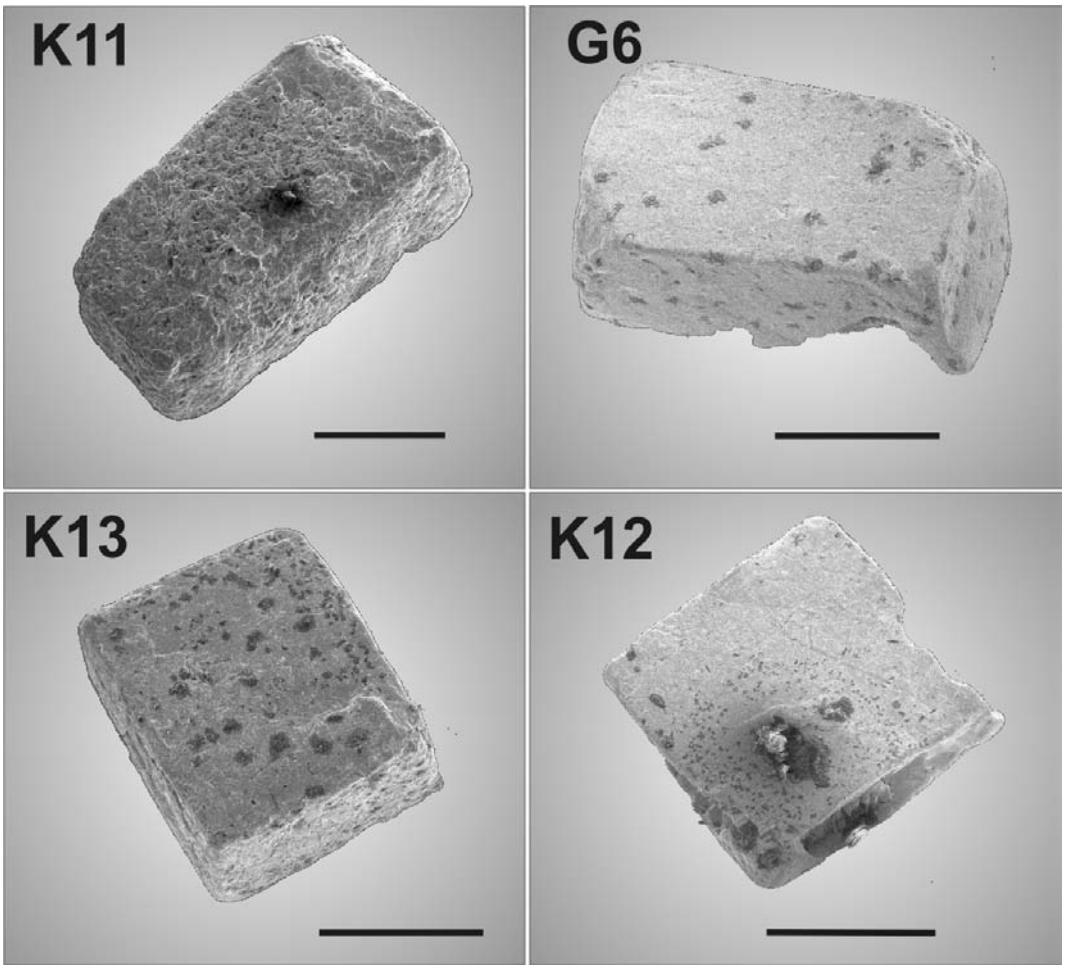

FIG. 4. SEM images of ferroan platinum crystals. Scale bar = 1 mm.

habit; one twinned crystal was also found (Fig. 4). The chemical composition corresponds to essentially pure Pt_3Fe with a compositional range from $Pt_{2.64}Fe_{1.00}$ to $Pt_{2.88}Fe_{1.00}$, and a minor copper component (up to 0.48 wt.%). Other PGE such as Os, Ru, Ir, Rh and Pd are below the analytical detection limit of the electron microprobe (0.10 wt.% for Os, 0.06 wt.% for Ru, 0.14 wt.% for Ir, 0.07 wt.% for Rh, and 0.14 wt.% for Pd) (Table 1).

The Pt-Fe alloy of Pt_3Fe composition occurs in two structural states, i.e. isoferroplatinum with a primitive cubic structure (space group *Pm*3*m*), and ferroan platinum with a face-centred cubic structure (space group *Fm*3*m*) (Cabri and Feather, 1975). We have taken powder diffraction diagrams from the Pt-Fe alloy in order to distinguish the cell type, but the strong texture in the samples prevented discrimination in this way. Therefore, we investigated a small piece of a crystal ($0.14 \times 0.11 \times 0.09$ mm) drilled from a polished section on a single-crystal diffractometer. Taking a rotation photograph, the complete diffracted powder rings can be displayed on the CCD-area detector avoiding the problems connected with texture. With a crystal-detector distance of 5 cm we thus recorded powder rings corresponding to Bragg-Brentano powder lines of 90º2θ Cu-$K\alpha$. The sample gave just four lines, which could be indexed with an F-centred lattice type with a cell constant of 3.86(1) Å. These are the lines expected for

TABLE 1. Selected analyses of ferroan platinum alloys.

Sample	K12	DR3	Dr5	Dr4	Dr2	Dr1
wt.%						
Pt	89.63	89.66	90.2	90.59	90.45	90.29
Fe	8.83	8.83	8.71	8.61	8.58	8.68
Cu	0.34	0.26	0.23	0.29	0.25	0.28
Total	98.80	98.75	99.14	99.49	99.29	99.25
at.%						
Pt	73.76	73.81	74.34	74.52	74.62	74.33
Fe	25.38	25.39	25.08	24.74	24.74	24.97
Cu	0.86	0.66	0.58	0.73	0.64	0.70
Total	100	100	100	100	100	100

Note: Ru, Rh, Os, Ir, Pd, S, Au, Ni, Sn, Sb, As were not detected

ferroan platinum alloy (Cabri and Laflamme, 1997). Thus, within the experimental limitations, XRD suggests that the Pt-Fe alloy from the Darya area has F-centred lattice type (Table 2).

Occasionally, the ferroan platinum crystals have cooperite overgrowth rims up to ~100 μm wide (Table 3, Fig. 5*b*) and contain μm-sized inclusions of bornite and minerals of the chalcocite group, probably digenite [Cu_9S_5] (Table 4). One sample is covered by a gold-rich Au-Ag alloy (Fig. 5*a*). Sulphates and K-bearing silicates are often attached to the surface of the ferroan platinum crystals.

Cooperite

Cooperite is also fairly common. It occurs both as large euhedral crystals (up to 3 mm across), partly twinned (Fig. 6), as overgrowth rims on Pt-Fe crystals and as intergrowth aggregates with mertieite-II. It has constant chemical composition and has no detectable impurities (Fe and Ni below detection limit), except an appreciable palladium content of up to 25 wt.% Pd (intergrowth with mertieite-II) (Table 3). Occasionally, it contains chalcopyrite inclusions (Table 4).

TABLE 2. XRD data for ferroan platinum.

hkl	a_o= 3.86(1) Å *d* value	Intensity
111	2.225	strong
200	1.935	medium
220	1.362	weak
311	1.164	weak

Mertieite-II

Palladium antimonides are also relatively abundant and occur in grain sizes from 1.3 to 2.5 mm (Fig. 7). The largest crystal (Sample K9) displays perfect hexagonal habit (Fig. 8*a*), and a sheetlike texture (Fig. 8*b*). It is brittle and shows perfect cleavage along (0001) (Fig. 8*c*). More than 60 analyses were performed on different grains of palladium antimonide (Table 5). The chemical data were recalculated based on known mineral stoichiometries, i.e. on the basis of 11 atoms for mertieite-II $Pd_8(Sb,As)_3$, on the basis of 15 atoms for mertieite-I $Pd_{11}(Sb,As)_4$-isomertieite $Pd_{11}Sb_2As_2$), and on the basis of 7 atoms for stibiopalladinite Pd_5Sb_2. A precise definition based on chemical composition only is difficult inasmuch as, according to Table 5 (including the control analyses for sample K9, done at CANMET, Ottawa), the grains could be mertieite-I, mertieite-II, or stibiopalladinite. The powder X-ray data of palladium antimonide did not allow us to clearly distinguish mertieite-I and mertieite-II (Table 6). In order to clarify this, small crystal fragments of the sample K9 were analysed by single-crystal diffractometry.

This method showed trigonal symmetry with cell constants of a = 7.528(1) Å and c = 43.029(1) Å in a hexagonal lattice, which clearly proves that sample K9 is mertieite-II.

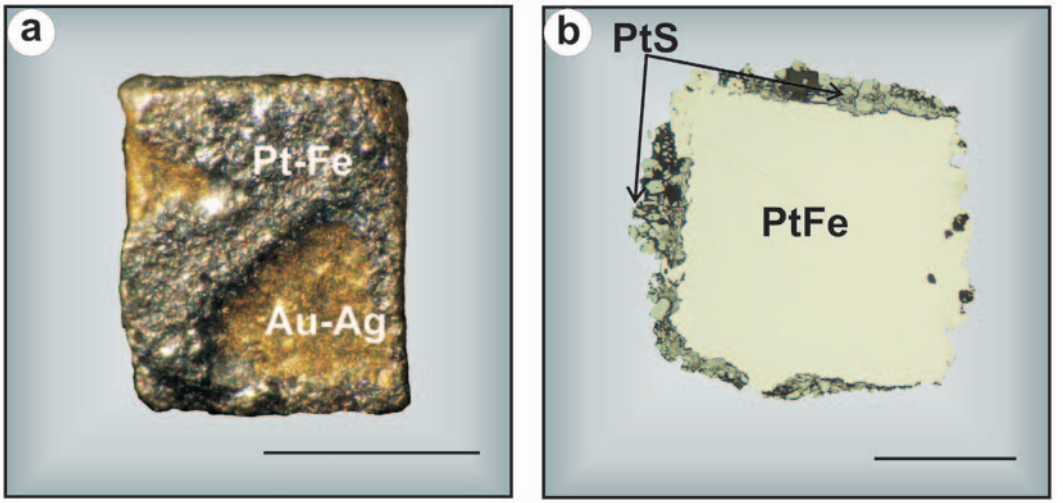

FIG. 5. Photomicrograph of Pt-Fe alloy crystals covered by (*a*) Au-Ag alloy (sample K2); (*b*) cooperite (sample Dr3). Scale bar = 1 mm.

The refinement of the structure was performed in space group $R\bar{3}c$ (167) and will be published soon (Bieniok *et al*., in prep.).

Two samples of palladium antimonide (Dr2 and K7) are dappled with μm-sized sperrylite inclusions, which are distributed irregularly in grain Dr2, and which are dispersed uniformly in K7, suggesting an exsolution fabric. In order to learn about the high-temperature composition, analysis of the palladium antimonide crystals was

TABLE 3. Selected analyses of cooperite-braggite and Pt-Pd-Hg phase.

	Cooperite-braggite								Pt-Pd-Hg	
Sample	G1m	G3m	Dr6m	K1-2r	Dr3r	K9r	K7	Dr2	Dr2	Dr2
no.	1	2	3	4	5	6	7	8	9	10
wt.%										
Pt	84.84	84.95	84.88	82.23	85.64	79.00	77.57	58.43	70.01	69.60
Pd	0.35	0.07	–	2.57	0.33	5.95	7.82	24.92	27.23	26.65
S	13.83	14.00	13.95	15.00	15.09	15.54	15.90	17.88	–	–
Fe	–	–	–	–	–	–	–	0.37	0.27	0.25
Hg	n.a.	n.a.	n.a.	n.a.	n.a.	n.a.	0.62	n.a.	3.56	3.24
Total	99.02	99.02	98.83	99.80	101.06	100.49	101.91	101.60	101.07	99.74
at.%										
Pt	50.02	49.90	50.00	46.15	48.10	42.83	40.99	27.28	56.31	56.83
Pd	0.38	0.08	–	2.64	0.34	5.91	7.57	21.33	40.15	39.89
S	49.60	50.03	50.00	51.21	51.56	51.26	51.12	50.79	–	–
Fe	–	–	–	–	–	–	–	0.60	0.76	0.71
Hg	n.a.	n.a.	n.a.	n.a.	n.a.	n.a.	0.32	n.a.	2.78	2.57
Total	100	100	100	100	100	100	100	100	100	100

Note: Au, Cu, Sn, Sb, As, Se were not detected; No 1–3 cooperite euhedral crystals, No 4–5 cooperite overgrowth on Pt-Fe crystals; No 6–8 intergrowth with mertieite-II
–: below detection limit
n.a.: not analysed

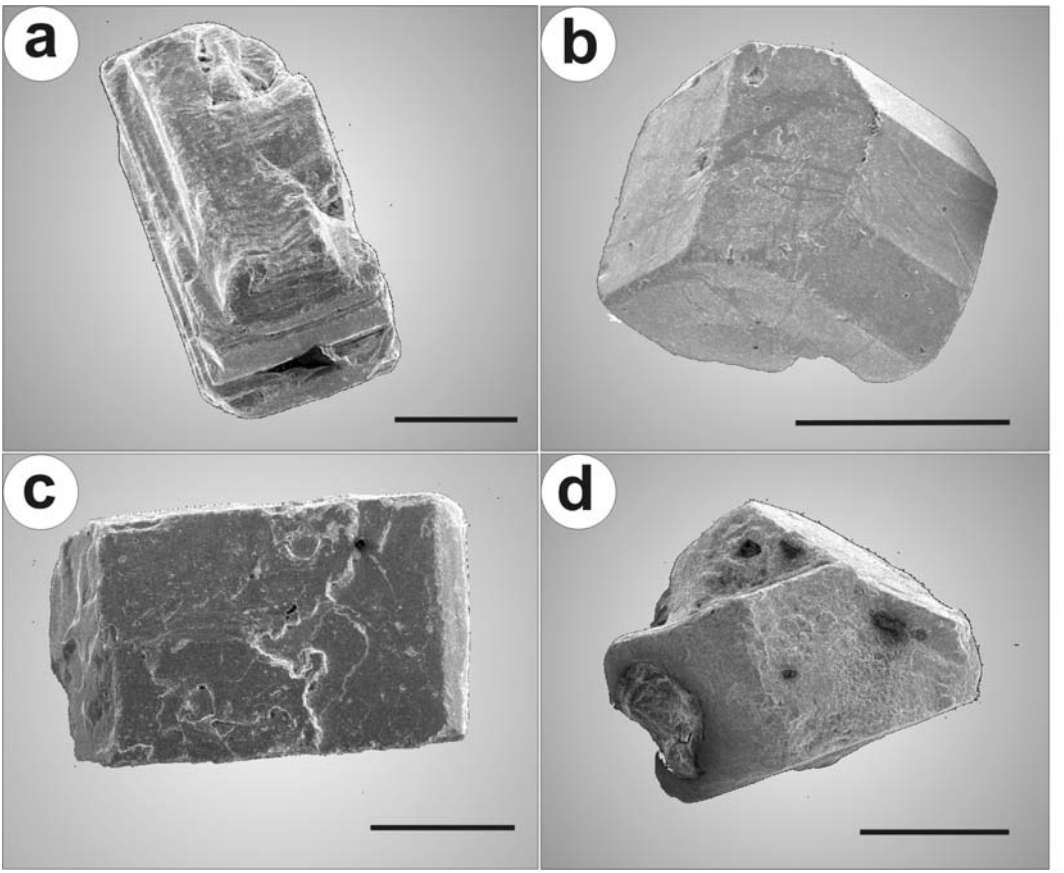

FIG. 6. SEM images of cooperite crystals (*a*–*c*) and cooperite twin (*d*). Scale bar = 1 mm. Samples: *a*–*c*: G3, K4, K1; *d*: G5.

performed with defocused beam (Ø = 50 μm). The primary composition of the K7 grain appears to be closer to stibiopalladinite whereas sample Dr2 could be interpreted both as mertieite-II and stibiopalladinite (Table 5). The better-preserved uniform exsolution texture in sample K7 makes the bulk analytical data for this sample more reliable, and one might speculate that the high-temperature primary state of both samples Dr2 and K7 was stibiopalladinite with a Pt content of up to ~5 wt.% Pt which then exsolved as sperrylite. A typical feature of the mertieite-II samples is the constant presence of tellurium as a trace element, with up to 2.64 wt.% Te in sample K9. Inclusions/intergrowths of keithconnite [Pd_3(Te,Bi)], (Pd,Pt)$_9$Te phase, Au-Ag alloy (Fig. 9), cooperite-braggite, Pt-Pd-Hg alloy (Fig. 10) are also typical features of the mertieite-II crystals.

Discussion

Euhedral crystals of PGM are often reported in the literature, but they commonly have a size not exceeding 200 μm. The relatively large PGM crystals from the Darya placer are highly unusual.

Due to the complexities of the Pd-Sb-As system with the occurrence of at least five different phases of similar chemical composition of $Pd_{8\pm x}(Sb,As)_{3\pm y}$, i.e. triclinic arsenopalladinite [$Pd_8As_{2.5}Sb_{0.5}$], cubic isomertieite [$Pd_{11}Sb_2As_2$], hexagonal mertieite-I [$Pd_{11}(Sb,As)_4$], rhombohedral mertieite-II [$Pd_8(Sb,As)_3$], and hexagonal stibiopalladinite [$Pd_{5+x}Sb_{2-x}$], it is difficult to determine precisely the mineral species found. The chemical data of Pd-Sb phases from the Darya river area are in favour of mertieite-II composition, although mertieite-I and stibiopalladinite cannot be excluded. The XRD analysis

TABLE 4. Composition of inclusions within the PGM crystals.

Mineral	Sperrylite	Chalcopyrite	Bornite	Chalcocite
No	1	2	3	4
wt.%				
Pd	0.37	–	–	–
Pt	53.74	2.56*	–	0.74*
Cu	–	34.50	68.80	74.09
Fe	–	29.49	7.21	2.28
S	–	33.42	23.84	21.42
Sb	0.15	–	–	–
As	43.11	–	–	–
Se	0.11	–	–	–
Total	97.48	99.98	99.85	97.79
at.%				
Pd	0.41	–	–	–
Pt	32.15	0.62	–	0.20
Cu	–	25.53	55.37	62.06
Fe	–	24.83	6.60	2.17
S	–	49.02	38.02	35.56
Sb	0.14	–	–	–
As	67.14	–	–	–
Se	0.16	–	–	–
Total	100	100	100	100

Note: Ru, Rh, Ag, Os, Bi, Au, Ir were not detected; –: below detection limit
No 1 is an inclusion within palladium antimonide; No 2 is an inclusion within cooperite, and Nos 3–4 are inclusions within ferroan platinum
* Because of the small size of these inclusions, it is assumed that the Pt content found in chalcopyrite and chalcocite is due to secondary fluorescence from the host minerals (cooperite and ferroan platinum).

obtained from sample K9 showed the mertieite-II structure, and the other three samples analysed, which have very similar chemical compositions, are also assumed to be mertieite-II.

Mertieite-II has been found in numerous PGE-bearing deposits as free grain concentrate, as inclusions or as complex intergrowths of 0.1–0.5 mm size (mostly <0.25 mm) (Cabri, 2002, and references therein; Cabral *et al*., 2002; Augé *et al*., 2002; Gervilla and Kojonen, 2002). The occurrence of an idiomorphic crystal of mertieite-II as a mm-sized crystal is first reported here. The minor changes in stoichiometry of the samples studied probably reflect the amount of As dissolved in mertieite-II which appears to be controlled by the amount of Pt in the high-temperature solid solution. None of the four grains studied (except sample K7, where three analyses out of 12 have a Pt content of up to 0.61 wt.%), showed even traces of Pt by spot analysis. However, bulk analysis suggests that the primary high-temperature solid solution incorporated up to ~5 wt.% Pt, which completely exsolved to sperrylite on cooling. The more Pt was in the primary solid solution the less As will be left within the palladium antimonide structure.

A remarkable and characteristic feature of the palladium antimonide crystals from the Darya placer are complex Pd-oxides along crystallographically controlled fractures. These Pd-oxides are relatively high (several wt.%) in Pt, Sb, Fe, Te, Bi, with traces of Sn, As and Cu. Some phases also contain Hg. Textural changes during microanalysis and low totals suggest the presence of H_2O/OH. The detailed study of these oxygenated compounds is a topic for future study.

Hg-bearing Pt-Pd-alloy has been detected very rarely so far. A very similar association of Hg-bearing Pt-Pd alloy with Pd-oxygenated compounds on isomertieite was previously

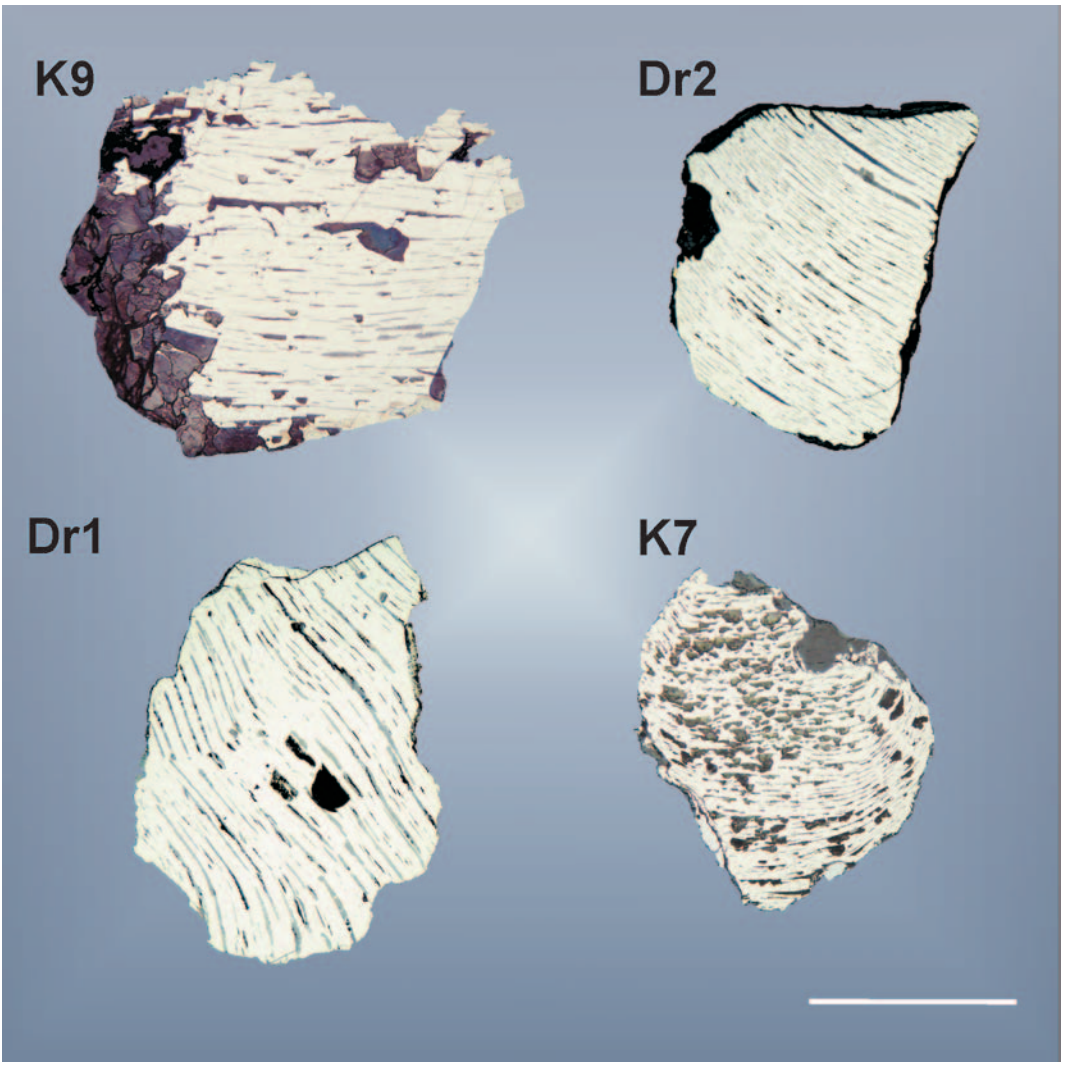

FIG. 7. Photomicrographs of mertieite grains. Note sheet-like grey phase of Pd-oxides along cleavage planes. Scale bar = 1 mm.

described by Cabral *et al*. (2002) from the Gongo Soco iron mine, Brazil. The authors suggested the formation from a low-temperature hydrothermal fluid. In the case of Darya samples the Pt-Pd-Hg grain was attached to mertieite-II and the cooperite-braggite. The compositional similarity of the latter to the Hg-bearing phase (note the very similar Pd content of cooperite and Pt-Pd-Hg phase: Table 3 Nos 8–10) allows us to assume that the Hg-bearing palladian platinum was formed as a result of hydrothermal alteration of a cooperite-braggite grain.

The Darya placer has two varieties of Pt-Fe alloy, also typical of the Kondyor placer (Nekrasov *et al*., 1994). The first and more abundant variant is small xenomorphic grains of Pt-Fe alloy (not studied here) and the second is relatively large ferroan platinum crystals. Mochalov (2001) reported on the lack of IPGE (refractory PGE) minerals in the Darya river, as well as on the low trace-element content of the xenomorphic grains of Pt-Fe alloy. The plot of average PGE distribution (Fig. 11) of xenomorphic Pt-Fe alloy from the Darya placer

TABLE 5. Average analyses of mertieite crystals.

wt.%	Dr1 *n* = 16	Dr2 *n* = 9	Dr2 defocused *n* = 6	K9 *n* = 11	K9* *n* = 18	K7 *n* = 12	K7 defocused *n* = 9
Pd	71.85±0.26	71.84±0.15	69.97±0.82	71.81±0.31	71.37±0.42	71.04±0.46	66.89±0.82
Sn	0.98±0.34	1.28±0.09	1.27±0.06	1.51±0.15	1.02±0.17	1.58±0.24	1.42±0.04
Sb	22.51±0.77	22.23±0.26	21.79±0.60	21.04±0.17	21.31±0.38	24.78±0.51	22.47±0.51
Pt	–	–	1.81±0.83	–	–	0.12±0.42	4.13±0.78
Te	0.85±0.06	0.67±0.09	0.82±0.12	2.01±0.20	2.16±0.20	0.44±0.30	0.72±0.13
As	3.8±0.24	3.26±0.12	4.31±0.81	3.62±0.11	3.83±0.18	2.3±0.39	4.80±0.70
Cu	n.a.	n.a.	n.a.	n.a.	0.18±0.02	n.a.	n.a.
Total	99.99±1.67	99.28±0.71	99.97±3.24	99.99±0.94	99.86±0.47	100.26±2.32	100.43±2.98
Calculation made on the basis of 11 atoms - mertieite-II $Pd_8(Sb,As)_3$ (a.p.f.u.)							
Pd	8.03 ±0.11	8.10±0.04	7.86±0.16	8.03±0.04	7.98±0.03	7.99±0.11	7.55±0.13
Sn	0.10 ±0.03	0.13±0.01	0.13±0.00	0.15±0.01	0.10±0.02	0.16±0.02	0.14±0.00
Sb	2.20±0.04	2.19±0.01	2.14±0.01	2.05±0.00	2.08±0.04	2.43±0.00	2.21±0.01
Pt	–	–	0.11±0.05	–	–	0.01±0.03	0.25±0.04
Te	0.08±0.01	0.06±0.01	0.08±0.01	0.19±0.02	0.20±0.02	0.04±0.03	0.07±0.01
As	0.60±0.03	0.52±0.02	0.69±0.11	0.57±0.01	0.61±0.03	0.37±0.04	0.77±0.09
Cu	–	–	–	–	0.03±0.00	–	–
Pd+Pt+Cu	8.03 ±0.11	8.10±0.04	7.97±0.11	8.03±0.04	8.01±0.03	8.00±0.09	7.80±0.09
Sn+Sb+ Te+As	2.97±0.11	2.90±0.04	3.03±0.11	2.97±0.04	2.99±0.03	3.00±0.09	3.20±0.09
Calculation made on the basis of 15 atoms - mertieite-I $Pd_{11}(Sb,As)_4$- isomertieite $Pd_{11}Sb_2As_2$							
Pd	10.94 ±0.14	11.04±0.06	10.71±0.22	10.95±0.06	10.88±0.05	10.89±0.16	10.29±0.18
Sn	0.13 ±0.04	0.18±0.01	0.17±0.00	0.21±0.02	0.14±0.02	0.22±0.03	0.20±0.00
Sb	2.99±0.05	2.98±0.01	2.91±0.01	2.80±0.00	2.84±0.05	3.32±0.00	3.02±0.02
Pt	–	–	0.15±0.07	–	–	0.01±0.04	0.35±0.06
Te	0.11±0.01	0.09±0.01	0.10±0.01	0.26±0.02	0.27±0.03	0.06±0.04	0.09±0.01
As	0.82±0.04	0.71±0.02	0.94±0.15	0.78±0.02	0.83±0.04	0.50±0.05	1.05±0.13
Cu					0.05±0.01		
Pd+Pt+Cu	10.94±0.14	11.04±0.06	10.86±0.15	10.95±0.06	10.92±0.05	10.90±0.12	10.64±0.12
Sn+Sb+ Te+As	4.06±0.14	3.95±0.06	4.14±0.15	4.05±0.06	4.08±0.05	4.10±0.12	4.36±0.12
Calculation made on the basis of 7 atoms - stibiopalladinite Pd_5Sb_2							
Pd	5.11±0.07	5.15±0.03	5.00±0.10	5.11±0.03	5.07±0.02	5.08±0.07	4.80±0.08
Sn	0.06±0.02	0.08±0.01	0.08±0.00	0.10±0.01	0.07±0.01	0.10±0.01	0.09±0.00
Sb	1.40±0.03	1.39±0.01	1.36±0.01	1.31±0.00	1.32±0.03	1.55±0.00	1.41±0.01
Pt	–	–	0.07±0.03	–	–	0.00±0.02	0.16±0.03
Te	0.05±0.00	0.04±0.01	0.05±0.01	0.12±0.01	0.13±0.01	0.03±0.02	0.04±0.01
As	0.38±0.02	0.33±0.01	0.44±0.07	0.37±0.01	0.39±0.02	0.23±0.0.3	0.49±0.06
Cu					0.02±0.00		
Pd+Pt+Cu	5.11±0.07	5.15±0.03	5.07±0.07	5.11±0.03	5.10±0.02	5.09±0.06	4.97±0.06
Sn+Sb+ Te+As	1.89±0.07	1.85±0.03	1.93±0.07	1.89±0.03	1.90±0.02	1.91±0.09	2.03±0.06

Note: S, Fe, Hg, Bi - below detection limit; n.a. not analysed
* Analysis done at Centre for Mineral and Energy Technology, Ottawa, Canada
For sample K9* Ni, Fe, Ir and Bi were sought but not detected.

TABLE 6. XRD data for mertieite-II, sample K-9.

No	º2θ	*d*	*I*	*hkl*
1	24.86	3.579	16	310
2	32.10	2.786	11	323
3	34.64	2.587	10	501
4	36.52	2.458	14	406
5	37.64	2.388	100	317
6	39.44	2.283	77	407
7	41.52	2.173	31	600
8	44.88	2.018	18	507
9	47.32	1.919	10	613
10	48.78	1.865	10	700
11	50.31	1.812	7	1112
12	50.92	1.792	12	607

shows a distribution pattern similar to Pt-Fe alloy from other zoned ultramafic-alkaline massifs of Alaskan-/Uralian-type.

Large (>1 mm across) Pt-Fe alloy crystals are very rare in nature. To our knowledge, the Kondyor PGE-Au placer is the only occurrence known so far. The euhedral Pt-Fe alloy from Kondyor consists of mm- to cm-sized ferroan platinum of F-centred cubic cell type (Cabri *et al*., 1997).

Our study reveals that all PGE besides Pt in the euhedral ferroan platinum crystals from Darya are below the electron-microprobe detection limit, similar to ferroan platinum crystals from Kondyor (Nekrasov *et al*., 1994; Cabri and Laflamme, 1997; Shcheka *et al*., 2004). Shcheka *et al*. (2004) studied Pt-Fe crystals from Kondyor by proton microprobe analysis and detected only 150 ppm

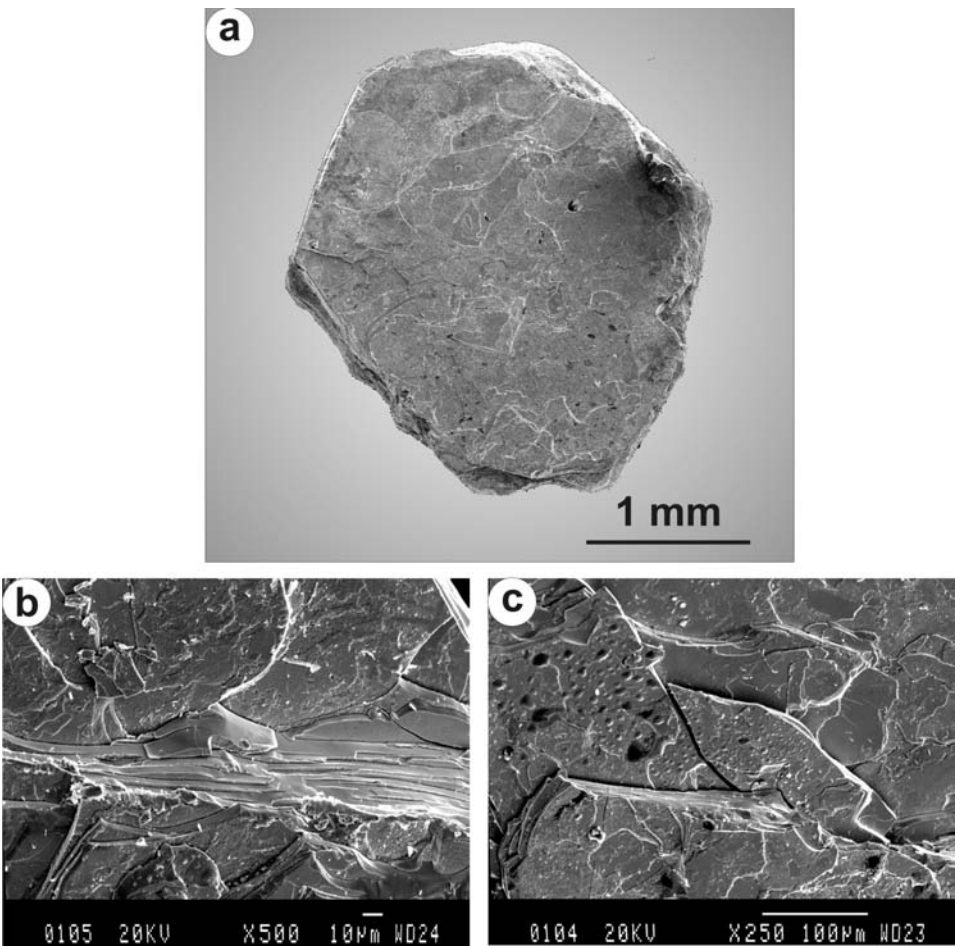

FIG. 8. SEM images of mertieite crystal: (*a*) general view; (*b*) higher magnification that highlights sheetlike texture; (*c*) fracture/cleavage pattern of the crystal. Sample K9.

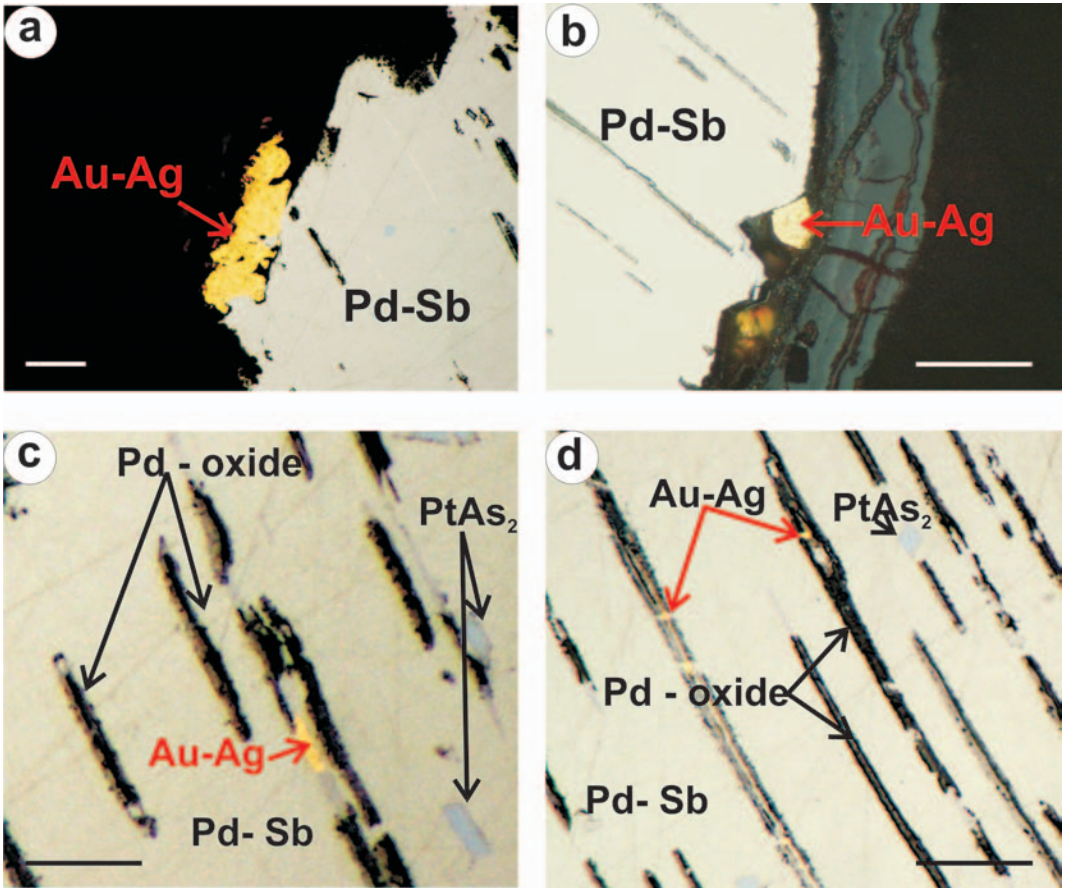

FIG. 9. Photomicrographs of Au-Ag intergrowth (*a*, *b*) and inclusions (*c*, *d*) within mertieite-II crystal. Oil immersion. Sample Dr2. Scale bar = 20 μm.

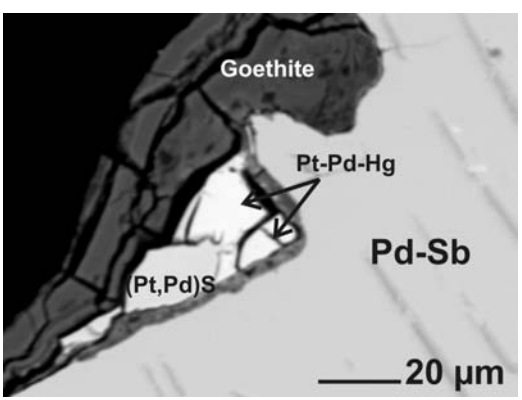

FIG. 10. BSE image of braggite intergrown with Pt-Pd-Hg attached to mertieite crystal. Sample Dr2.

Pd, 100 ppm Rh and 20 ppm Ru. Osmium and Ir were below the analytical detection limit of the electron microprobe (1500 ppm), and the PIXE method did not allow analysis for these elements due to overlap of the Os and Ir *L* lines with the Pt *L* lines. The earlier SIMS study by Cabri *et al*. (1998) gave <1 ppm Os. Cabri and Laflamme (1997) pointed out that 99.8% of >1700 Pt-Fe analyses collected by Cabri *et al*. (1996) always have traces of Ir, Os and Rh. Therefore, the lack of detectable PGE in ferroan platinum crystals from both Kondyor and Darya is a remarkable chemical signature which probably reflects uncommon conditions of crystallization in these two localities. The lack of IPGE minerals in the mineral assemblage from the Darya placer indicates early PGE fractionation, which had probably already taken place during early stages

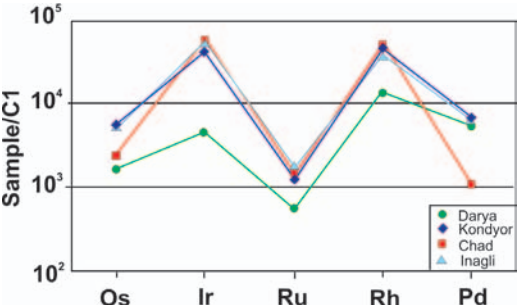

FIG. 11. Chondrite-normalized PGE distribution of xenomorphic Pt-Fe alloy from the Darya placer compared to xenomorphic Pt-Fe alloys from the Kondyor, Inagli and Chad placers (based on data from Mochalov, 2001).

of melt crystallization. The lower the temperature, the fewer PGE that can enter the structure of Pt-Fe alloy. It appears likely that the temperature of formation of the large PGM crystals from the Darya and Kondyor placers was considerably lower than the temperature of average xenomorphic fine-grained Pt-Fe alloy from the same intrusions. The Au-Ag rims on the ferroan platinum crystals and intergrowth aggregates with mertieite-II suggest hydrothermal overprint, as also seen for the Pt-Fe alloy crystals from Kondyor (Shcheka *et al*., 2004). Medium- to coarse-grained pegmatoidal clinopyroxenite bodies are associated both with the Darya and Kondyor PGM occurrences. The formation of the large euhedral PGM crystals could be related to residual pegmatitic fluids at much lower temperature than common in magmatic PGE deposits. A similar situation applies to the Tweefontein area, South Africa, where large euhedral crystals of sperrylite up to 1.85 cm across occur in granite pegmatite and on shear zones in ironstone country-rocks of the Platreef (Wagner, 1929).

Acknowledgements

The authors are grateful to Prof. Louis J. Cabri (Ottawa) for his interest in this paper, help with control analysis of sample K9, and careful editing of the paper; Prof. Sergej A. Shcheka (Vladivostok) is thanked for his constructive remarks on the manuscript; Dr. Andrew McDonald (Sudbury) for help with interpretation of X-ray data; Klaus Herrmann, Eike Gierth and Frank Sandhagen (Clausthal), for excellent technical support during the electron microprobe analysis and scanning electron microcopy, respectively; Svyatoslav Shcheka (Tübingen) for the help with carrying out the X-ray powder analysis of mertieite-II; and Ulf Hemmerling and Fred Türck (Clausthal) for sample preparation and computer support, respectively.

References

Augé, T., Salpeteur, I., Bailly, L., Mukherjee, M. and Patra, R.N. (2002) Magmatic and hydrothermal platinum-group minerals and base-metal sulfides in Baula complex, India. *The Canadian Mineralogist*, **40**, 277–309.

Cabral, A.R., Lehmann, B. Kwitko, R. and Jones, R.D. (2002) Palladian gold and palladian arsenide-antimonide minerals from Gongo Soco iron ore mine, Quadrilátero Ferrífero, Minas Gerais, Brazil. *Transactions of the Institution of Mining and Metallurgy, Section B: Applied Earth Science*, **111**, B74–B80.

Cabri, L.J. (2002) The platinum-group minerals. *The Geology, Geochemistry, Mineralogy and Mineral Beneficiation of Platinum-group Elements* (L.J. Cabri, editor). Canadian Institute of Mining, Metallurgy and Petroleum, Special Volume, **54**, 13–129.

Cabri, L.J. and Feather, C.E. (1975) Platinum-iron alloys: a nomenclature based on a study of natural and synthetic alloys. *The Canadian Mineralogist*, **13**, 117–126.

Cabri, L.J. and Laflamme, J.H.G. (1997) Platinum-group minerals from the Konder Massif, Russian Far East. *The Mineralogical Record*, **28**, March–April, 97–106.

Cabri, L.J., Harris, D.C. and Weiser, T.W. (1996) Mineralogy and distribution of platinum mineral (PGM) placer deposits of the world. *Exploration Mining Geology*, **5**, 73–167.

Cabri, L.J., Stern, R.A. and Czamanske, G.K. (1998) Osmium isotope measurements of Pt-Fe alloy placer nuggets from the Konder intrusion using a Shrimp II ion microprobe. *8th International Platinum Symposium*, Abstracts, pp. 55–58.

El'yanov, A.A. and Andreev, G.B. (1991) *Magmatism and Metallogeny of the Platform Provinces of Multistage Activation.* Nauka, Novosibirsk, 168 pp. (in Russian).

Gervilla, F. and Kojonen, K. (2002) The platinum-group minerals in the upper section of the Keivitsansarvi Ni-Cu-PGE deposit, Northern Finland. *The Canadian Mineralogist*, **40**, 377–394.

Gurovitch, V.G., Zemlyanukhin, V.N., Emelyanenko, E.P., Karetnikov, A.S., Kvasov, A.I., Lazarenkov, V.G., Malitch, K.N., Mochalov, A.G., Prikhod'ko, V.S. and Stepashenko, A.A. (1994) *Geology,*

Petrology and Ore Presence of the Kondyor Massif (Yu.A. Kosigin and V.S. Prikhod'ko, editors). Nauka, Moscow, 176 pp. (in Russian).

Malitch, K.N. (1999) *Platinum-group Elements in Clinopyroxenite-dunite Massifs of East Siberia (Geochemistry, Mineralogy, and Genesis).* Saint Petersburg Cartographic Factory VSEGEI Press, St. Petersburg, 296 pp. (in Russian).

Malitch, K.N. and Thalhammer, O.A.R. (2002) Pt-Fe nuggets derived from clinopyroxenite-dunite massifs, Russia: a structural, compositional and osmium-isotope study. *The Canadian Mineralogist,* **40**, 395–418.

Mochalov, A.G. (2001) *'Heavy concentrate platinum' from the placers of the Russian Far East.* Abstract of doctoral thesis. IGEM, Moscow, 48 pp. (in Russian)

Nekrasov, I.Ya, Lennikov, A.M, Oktyabrsky, R.A., Zalishchak, B.L. and Sapin, B.I. (1994) *Petrology and Platinum Mineralization of the Alkaline-ultramafic Ring Complexes* (N.P. Laverov, editor). Nauka, Moscow, 381 pp. (in Russian).

Pushkarev, Yu.D., Kostoyanov, A.I., Orlova, M.P., and Bogomolov, E.S. (2002) Peculiarities of the Rb-Sr, Sm-Nd, Re-Os and K-Ar isotope systems in the Kondyor massif: mantle substratum, enriched by PGE. *Regional Geology and Metallogeny,* **16**, 80–91 (in Russian).

Rozhkov, I.S., Kitsul, V.I., Razin, L.V. and Borishanskaya, S.S (1962) *Platinum of Aldan Shield*. Academy of Sciences of the USSR Press, Moscow, 119 pp. (in Russian).

Shcheka, G.G., Lehmann, B., Gierth, E., Goemann, K. and Wallianos, A. (2004) Macrocrystals of Fe-Pt alloy from the Kondyor PGE placer deposit, Khabarovskiy Kray, Russia: Trace element content, mineral inclusions and reaction assemblages. *The Canadian Mineralogist*, **42**, 601–617.

Sushkin, L.V. (1995) Characteristic features of the native elements of the Kondyor deposit. *Tikhookeanskaya Geologiya*, **14**, 97–102 (in Russian).

Szymañski, J.T., Cabri, L.J. and Laflamme, J.H.G. (1997) The crystal structure and calculated powder-diffraction data for zvyagintsevite, Pd_3Pb. *The Canadian Mineralogist*, **35**, 773–776.

Wagner, P.A. (1929) *The Platinum Deposits and Mines of South Africa.* Oliver and Boyd, London, 326 pp.

[*Manuscript received 13 September 2004: revised 18 October 2004*]